# Buckling of Imperfect Stiffened Cylindrical Shells under Axial Compression

JOSEF SINGER,* JOHANN ARBOCZ,† AND CHARLES D. BABCOCK, JR.‡
*California Institute of Technology, Pasadena, Calif.*

**Axial buckling tests on machined integrally stiffened cylindrical shells were carried out. Complete mappings of the shell imperfections and the prebuckling growth were obtained. The lightly ring-stiffened shells behaved in a manner similar to the isotropic shells that were previously tested. For these shells, the predominant prebuckling deformation consisted of a half-wave in the axial direction with several circumferential waves. The similarity of the lightly ring-stiffened shells and the isotropic ones suggests that the uniqueness of the buckling mode for stiffened shells may not greatly influence the prebuckling behavior. The heavily ring-stiffened shells showed a sizable amount of short wave length axisymmetric growth before buckling. Buckling in all cases resulted in an asymmetric pattern. The stringer-stiffened shells showed a prebuckling behavior also similar to the isotropic results. However, the buckling pattern consisted of longer axial wave lengths. Correlation of the experimentally obtained buckling loads with linear buckling theory showed good agreement in most cases.**

## Nomenclature

| | | |
|---|---|---|
| $A_1,A_2$ | = | stiffener area, ring area, respectively |
| $AR,AS$ | = | aluminum shells, ring-stiffened and stringer-stiffened |
| $BR,BS$ | = | brass shells, ring-stiffened and stringer-stiffened |
| $C_{mn}$ | = | harmonic component; Eq. (2) |
| $D_{mn}$ | = | harmonic component; Eq. (2) |
| $d$ | = | distance between stiffeners |
| $E$ | = | Young's modulus |
| $e$ | = | distance between centroid of stiffener cross section and middle surface shell, negative when outside |
| $H$ | = | stiffener height |
| $I$ | = | moment of inertia of stiffener cross section about its centroidal axis |
| $L$ | = | length of shell |
| $M_x$ | = | moment resultant |
| $m$ | = | axial half-wave number |
| $N_x,N_{xy}$ | = | membrane force resultant |
| $n$ | = | circumferential wave number |
| $P_{cl}$ | = | classical buckling load $P_{cl} = 2\pi Et^2/[3(1-\nu^2)]^{1/2}$ |
| $P_R$ | = | buckling load for ring stiffened shells |
| $q$ | = | number of rings |
| $R$ | = | radius of shell |
| $t$ | = | thickness of shell |
| $u$ | = | axial displacement |
| $v$ | = | circumferential displacement |
| $w$ | = | radial displacement |
| $\bar{w}$ | = | radial imperfection from perfect circular cylinder |
| $x,y$ | = | axial and circumferential coordinates on middle surface of shell, respectively |
| $Z$ | = | shell parameter $[(Z = (1-\nu^2)^{1/2}(L/R)^2(t/R))]$ |
| $\nu$ | = | Poisson's ratio |

## Introduction

CONSIDERABLE research efforts have been directed in recent years to the study of the influence of initial imperfections on the buckling of cylindrical shells. Though in-plane boundary conditions and prebuckling deformations were shown by many investigators[1,2] to affect buckling appreciably, initial imperfections have been identified as the main cause of the large discrepancies between experimental and theoretical buckling loads of unstiffened cylindrical shells under axial compression. For closely stiffened shells, the influence of the imperfections is less pronounced and the predictions of linearized classical theory are much closer to test results.[3] The initial imperfections remain, however, the main degrading factor and hence, warrant extensive study if one aims at the development of reliable methods for determining the reduction of buckling loads.

The imperfection sensitivity concept introduced by Koiter[4,5] presented a powerful analytical tool that has recently been extensively used.[6-9] These analyses restrict the initial imperfections to linearized buckling modes, which implies the assumption that only these components of the initial imperfections will be amplified. For isotropic cylindrical shells under axial compression, however, other imperfection components were observed to grow as rapidly,[10] indicating a necessity for extension of the analysis to include also modes of imperfection which do not correspond to the lowest buckling modes of linearized theory. Such an analysis[10] with a simplified model of "pairs of critical modal components," pairs consisting of an axisymmetric component and an asymmetric one, yielded encouraging agreement with experimental buckling loads. The study of the growth of the initial imperfections in Ref. 10 showed that for isotropic cylindrical shells under axial compression, a long wave axisymmetric component of the initial imperfection (that does not correspond to the lowest buckling mode of linearized theory) was important in causing the shell to buckle below the classical value. Though axisymmetric imperfections alone (corresponding to the axisymmetric buckling mode of the perfect shell) were shown by Koiter[6] to reduce the buckling load of unstiffened cylindrical shells drastically, the coupling of axisymmetric and asymmetric components of general initial imperfections may be the reason for the wide scatter and low buckling loads obtained in practice.

For closely stiffened shells, the reduction in buckling loads and the scatter of test results is less severe. One may therefore suspect that the prebuckling behavior of stiffened cylindrical shells will differ. Hence, the main purpose of the present work was to study the growth of the initial imperfections and buckling behavior in integrally machined ring- and stringer-stiffened cylindrical shells under axial compression,

Received June 5, 1970. The authors wish to express their appreciation to E. E. Sechler for his encouragement and help in carrying out the work reported in this paper. This work was supported in part by the Sloan Foundation and this aid is gratefully acknowledged.

* Visiting Professor of Aeronautics, 1968–1969; presently Professor, Department of Aeronautical Engineering, Technion, Israel Institute of Technology, Haifa, Israel. Associate Fellow AIAA.

† Research Fellow; also Associate Professor of Aeronautics, Northrop Institute of Technology.

‡ Associate Professor of Aeronautics. Associate Member AIAA.

and compare them with the results obtained for isotropic shells. For tracing the growth of imperfections, the special test rig developed at GALCIT[10] with an automated scanning noncontact probe is used, after conversion of the system to capacitance type pickups. The imperfection surveys are then decomposed into dominant components for correlation with the buckling modes.

Earlier experimental studies on the buckling of stiffened cylindrical shells[3,11-14] lead to the conclusion[3] that classical linear theory is applicable to closely stiffened cylindrical shells under axial compression, as a first approximation, with the same reliability as for isotropic shells under external pressure. This conclusion was recently reconfirmed by a parallel test program at the Technion.[15] The second purpose of the present test was to obtain further confirmation to this conclusion.

## Theoretical Considerations

If one assumes that classical linear theory predicts the buckling loads adequately, the analytical tools are readily available. For closely spaced stiffening, the general instability of stiffened cylindrical shells can be analyzed with a simple theory in which stiffeners are "smeared," or "distributed," over the entire shell, taking into account the eccentricity of the stiffeners.[16,17] This theory has been used by many investigators because of its simplicity, but other analyses are also available. Improved theories that consider also different in-plane boundary conditions, Refs. 18 and 19, and a general computer program, based on a finite difference solution, for shells or revolution with different types of stiffening, the BOSOR program, has been developed.[20] The discreteness of the stiffeners has usually a negligible effect (see Refs. 21 or 22 except for special cases[23]) but its influence can be readily verified by the method given in Ref. 22.

The simple linear smeared theory analysis for general instability under axial compression is presented in detail in Ref. 17 and summarized in Ref. 3. For ring-stiffened cylinders nonaxisymmetric buckling will occur with inside rings and the corresponding positive eccentricity will lower the buckling load below that for centrally placed rings. With outside rings, however, the increase in buckling load that would result from the negative eccentricity if the shell were to buckle in a chess board pattern is not realized, since the shell now buckles in the axisymmetric mode (ring-shape pattern) which is unaffected by eccentricity and yields a lower buckling load. Hence for outside rings, the general instability load can be computed from a simple formula if the axial wave number is treated as a continuous variable.

$$P_R = [3(1 - \nu^2)]^{-1/2} 2\pi t^2 E[1 + (A_2/dt)]^{1/2} = P_{cl}[1 + (A_2/dt)]^{1/2} \quad (1)$$

Though Eq. (1) is a good approximation, a more accurate $P_R$ is used for comparison with the experimental results. It should be pointed out, however, that though the axisymmetric mode is the lowest buckling mode for outside rings, the buckling load for the lowest asymmetric buckling mode is only slightly higher for weak and medium stiffening. This will be re-emphasized in the discussion of the test results, since it influences the behavior of imperfect shells.

For stringer-stiffened shells the same approach[17] is employed, but since axisymmetric buckling modes can occur only for very short shells, simple approximations similar to Eq. (1) are not feasible. It should also be remembered that the eccentricity and boundary condition effects in stringer-stiffened shells are much larger than those in ring-stiffened ones.

The classical linear theory for shell buckling assumes that the prebuckling state consists of the membrane stress state. This means that any prebuckling deformation due to the end constraints is neglected. In addition, the boundary conditions during buckling are assumed to be simple support (*SS*-3, $w = v = M_x = N_x = 0$). For the isotropic shell under axial compression, the effect of more rigid boundary conditions (for instance *C*-4, $w = w_{,x} = u = v = 0$) has been shown to be negligible.[1] For ring-stiffened cylindrical shells the effect of in-plane boundary conditions as well as rotational restraint (clamping) is similar to that observed in isotropic shells. The "weak in shear" boundary conditions *SS*1 and *SS*2 (with $N_{xy} = 0$ instead of $v = 0$) that rarely occur in practice, reduce the buckling load to about half the classical value; whereas axial restraint ($u = 0$ instead of $N_x = 0$) has a negligible effect yielding practically identical results for *SS*3 and *SS*4.[19] As in unstiffened shells, rotational restraint ($w_{,x} = 0$ instead of $M_x = 0$) increases the buckling load only for short shells, though here the influence extends to larger $Z$ values up to $Z = 100$.[18]

For stringer-stiffened shells, both rotational restraint and inplane boundary conditions are more important in particular with external stringers.[18,24] Rotational restraint is a major factor that may raise the buckling load in practical stringer-stiffened shell to more than twice its unrestrained value. Also, axial constraint affects results appreciably.

Nonlinear prebuckling deformations of the perfect shell were shown to have only a small effect on the buckling load of clamped isotropic cylindrical shells.[25] For ring-stiffened cylinders under axial compression, the effect was also found to be small.[26] A similar small effect was observed for ring-stiffened corrugated cylinders,[23] and also for stringer-stiffened shells the effect was found to be small.[27] As shown later, the observations are confirmed by calculations for the shells of the present paper. A similar conclusion was also reached recently by Kobayashi[28] for certain types of orthotropic shells. Hence, nonlinear prebuckling deformations are not a major factor in the determination of buckling load of stiffened cylindrical shells. However, it should be emphasized that the influence of nonlinear prebuckling deformation and the effect of boundary conditions should be investigated for the experimental conditions. Only then can it be said with confidence that the discrepancy between theory and experiment is due to some other factor such as initial imperfections.

Since the present study is concerned with the general instability of stiffened shells, local buckling between rings or stringers represents mainly a design constraint. Local buckling should not be critical at loads below the general instability load of the specimens. On the other hand, since for structural efficiency local buckling and general instability loads should not be far apart, the behavior of specimens for which these two modes of failure are close is also of interest. Local buckling is discussed in detail in Ref. 3 and two design implications emerge. First, the dimensions of the subshell or panel between stiffeners have to ensure its being in the range where classical buckling behavior occurs. Furthermore, the stiffening due to "shortness" of the subshell or "narrowness" of the panel predicted by classical linear theory must be at least equivalent to the stiffening of the shell by its stiffeners, as predicted by linear theory. For rings, this implies short subshells that would buckle locally well in the axisymmetric range, where imperfection sensitivity is very low, and for stringers this means narrow panels in the range where "plate type" buckling behavior dominates.[29]

The discreteness effect of rings in closely stiffened cylindrical shells under axial compression can usually be neglected.[3,21-23] However, if the number of rings in the test specimens is very close to the number of axial half-waves in the predicted axisymmetric buckle pattern, a recheck on the discreteness effect should be made. This can be readily accomplished with the type of analysis described in Ref. 22.

The consideration of initial imperfections has been greatly facilitated by the technique introduced by Koiter.[4-6] This type of methodology for imperfection sensitivity analysis has been pushed vigorously by Budiansky and Hutchinson

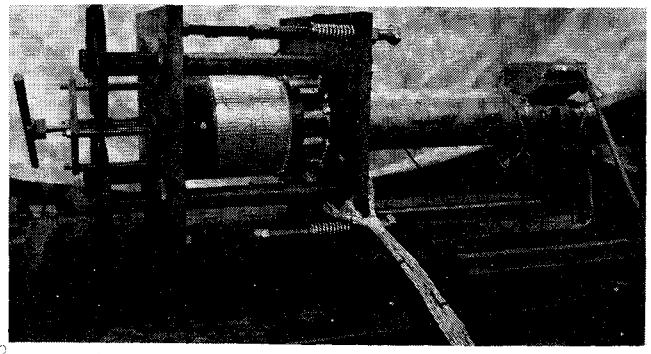

**Fig. 1 Testing machine with stringer-stiffened shell.**

and their group.[7-9] In their studies, the load is expanded in a series in terms of powers of the maximum lateral buckling deflection for a given shell loading configuration. For stiffened shells characterized by symmetrical postbuckling behavior the load displacement relation is given by

$$P/P_{cl} = 1 + b(\delta/t)^2$$

where $P_{cl}$ = classical buckling load; $\delta$ = amplitude of the buckling displacement; and $t$ = shell thickness. The coefficient $b$ is then a measure of the rapidity with which the load rises or drops after buckling. Carrying out the same type of analysis considering imperfections it is found that $b$ determines the decrease in load expected with an imperfection of magnitude $\bar{\delta}$. Imperfection sensitive structures are characterized by negative values of $b$.

Unfortunately, the manner in which the imperfection sensitivity coefficient $b$ can be utilized in the design of shell structures has not yet been established. Of even more immediate concern is the question as to the relevance of the coefficient as thus far established.

Imperfection sensitivity studies for stiffened cylindrical shells[9,30,31] showed, that though they appear to be less sensitive than isotropic cylinders, their sensitivity is still appreciable. The predicted sensitivities appear to depend strongly also on the assumptions regarding quantities that affect the classical buckling load only slightly (torsional stiffness of stiffeners and prebuckling deformations). The predicted regions of large imperfection sensitivity shift accordingly from one study[9] to another[31] and have not been borne out by experiment.[15] Hence these predictions cannot yet be relied upon.

The imperfection sensitivity predicted by these and other studies depends also very much on the assumed dominant initial imperfection. Axisymmetric imperfections in particular have been extensively studied since Koiter's pioneering work,[6] recently also experimentally.[32] However, since in practice imperfections of a more general shape are present, the effect of axisymmetric ones is only a partial indication of actual behavior. Hence, the approach of Ref. 10 that starts with measured general initial imperfections and studies their growth, is now employed for stiffened shell. The important question is, if and when are the linearized buckling modes the only important components of initial imperfections in stiffened shells?

## Test Apparatus and Specimens

The experimental program called for a scanning device with the capability of picking up and recording imperfections of only fractions of the test specimen's wall thickness. In addition, the scanning device had to travel both in the axial and in the circumferential directions in order to record a complete surface map of the shell being tested.

Such a scanning device was built around a noncontacting reluctance pickup which measured the distance between the end of the pickup and the metal surface of the shell. The pickup was installed in a movable support at the end of a long shaft which protruded inside the shell being tested. The shaft was moved in the axial and circumferential directions by small electric motors. The scanning sequence, consisting of a circumferential scan followed by an axial advance was controlled by strategically placed microswitches. The controlled end displacement type testing machine, scanning mechanism and a stringer-stiffened shell are shown in Fig. 1. When carrying out the imperfection measurements the output of the pickup was monitored on a digital voltmeter whose readings were recorded during the circumferential scans at preset intervals on punched cards. The output of the pickup was also displayed on an $XY$ plotter which afforded a constant surveillance of the test and an instant warning if a breakdown in the equipment occurred. Details of the equipment checkout procedure were presented in Ref. 10.

The previous work,[10] carried out with the scanning device just described, used a reluctance-type pickup developed in the GALCIT electronic shop. The initial work on the stiffened shell showed the eddy currents generated by this pickup penetrated into the surface being measured to a greater depth than previously thought. The stiffeners on the shell exterior significantly affected the displacement readings. Therefore, a capacitance-type pickup was developed for use with the same data acquisition system. However, the capacitance pickup was less stable than the reluctance pickup. This was overcome to some degree by controlling the temperature of the testing room and the electronic equipment. In addition, a pickup calibration was performed immediately prior to and after each buckling test. It was found that at the far end of the pickup range, there was some change in the calibration curve. However, since the measurements were made with the pickup close to the shell wall, this did not substantially affect the results. Several sets of shell data were reduced with the pretest and post-test calibration curves and the difference in prebuckling growth was insignificant for the two different calibration curves.

The ring- and stringer-stiffened aluminum shells were cut from 6061-T6 alloy tubing. The inside was first machined to the proper dimension and then the tube was placed on a steel mandrel by heating the aluminum about 100°F. The outside was then machined to the proper shape. The stringers were cut using an indexing head with a milling machine. The brass shells were cut in the same manner except that a fusible mandrel was used to support the shell during the outside machining. The geometry of the ring and stringer stiffened shells is shown in Fig. 2.

The machined shells were extensively measured in order to best determine the proper skin thickness and stiffener properties. The skin thickness is the smallest dimension and is subject to the largest error. Unfortunately, it is also one of the most sensitive parameters in determining the load carrying capacity of the shell, since the buckling load is roughly proportional to the skin thickness squared. The thickness was determined in two different manners. First, the thick-

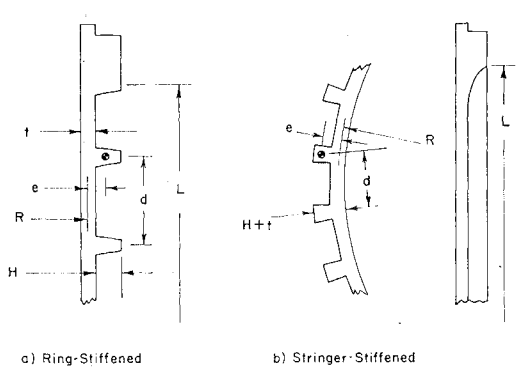


**Fig. 2 Geometry of stiffened shells.**

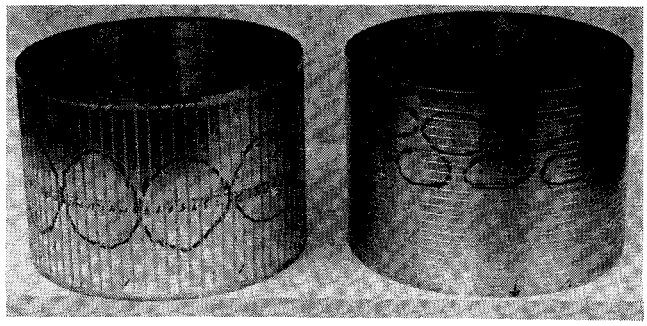

**Fig. 3 Postbuckling patterns for ring- and stringer-stiffened shells.**

ness was directly measured using a micrometer and an average of all readings found. In addition to this, each ring on the ring-stiffened shells was measured using an optical comparator. From these measurements, the total volume and weight for the rings could be accurately determined. Knowing the total weight of the shell, the average wall thickness was then calculated. For the ring-stiffened shells, this thickness by weight differed from the average micrometer readings by up to $0.44 \times 10^{-3}$ in. ($-0.44 \times 10^{-3}$ for *AR*-5, $0.30 \times 10^{-3}$ for *AR*-2).

For the stringer-stiffened shells the weight calculation was performed by carefully measuring the shell thickness before cutting the stringers and subtracting out the weight of the material cut to form the stringers. The unknown in this calculation is the depth of the cut. The resultant skin thickness agreed with the average micrometer reading to within one half of one percent. For both the ring- and stringer-stiffened shells, the thickness used in the theoretical calculations is the one obtained from the weight measurements.

The variation in the thickness for the test shells was obtained from the micrometer readings. The aluminum ring-stiffened shells all had a difference between the maximum and minimum thickness of $10^{-3}$ in. or less. Several shells were better than this by a factor of two. The brass shells that were tested were also within this tolerance. However, for several of these shells that were not tested, the difference was considerably greater. The stringer-stiffened shells showed a difference between maximum and minimum thickness up to $2 \times 10^{-3}$ in. in a few locations.

The geometric and material properties for the shells are shown in Table 1. The stiffeners are not rectangular in all cases and the measured shape is used in the calculation of stiffener properties. The skin thickness for the stringer-stiffened shells is an average thickness since the outside surface is composed of straight lines made by the cutter.

## Test Results and Discussion

The buckling tests were carried out in a manner identical to the isotropic shell tests previously reported.[10] After the shell was installed in the testing machine, the pickup calibration was performed and an initial scan was taken. The load

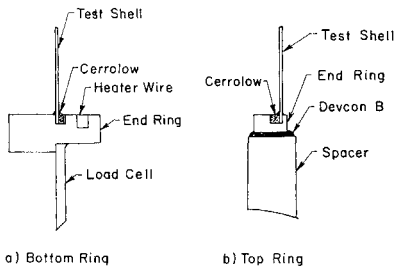


**Fig. 4 End rings for buckling tests.**

**Table 1 Geometric and material properties of test shells[a]**

| Shell | $t \times 10^3$ | $R/t$ | $L/R$ | $A/dt$ | $-e/t$ | $I/dt^3$ | $d$ | $L$ | No. of stiffeners |
|---|---|---|---|---|---|---|---|---|---|
| Aluminum Alloy | | | | | | | | | |
| *AR*-1 | 9.29 | 431 | 1.31 | 0.205 | 1.13 | 0.0288 | 0.250 | 5.25 | 20 |
| *AR*-2 | 9.50 | 421 | 1.31 | 0.198 | 1.11 | 0.0262 | 0.250 | 5.25 | 20 |
| *AR*-3 | 10.05 | 398 | 1.31 | 0.305 | 1.55 | 0.1287 | 0.250 | 5.25 | 20 |
| *AR*-4 | 10.43 | 384 | 1.31 | 0.293 | 1.52 | 0.1189 | 0.250 | 5.25 | 20 |
| *AR*-5 | 8.38 | 477 | 1.31 | 0.315 | 1.54 | 0.1266 | 0.250 | 5.25 | 20 |
| *AR*-6 | 8.46 | 473 | 1.31 | 0.307 | 1.51 | 0.1160 | 0.250 | 5.25 | 20 |
| *AR*-7 | 8.26 | 484 | 1.44 | 0.248 | 1.43 | 0.0738 | 0.320 | 5.76 | 17 |
| *AR*-9 | 8.32 | 481 | 1.38 | 0.678 | 2.88 | 1.6326 | 0.250 | 5.50 | 21 |
| *AR*-10 | 8.80 | 455 | 1.38 | 0.630 | 2.78 | 1.3711 | 0.250 | 5.50 | 21 |
| *AR*-11 | 8.13 | 492 | 1.35 | 0.777 | 2.63 | 1.5527 | 0.200 | 5.40 | 26 |
| *AR*-12 | 10.43 | 384 | 1.40 | 0.575 | 2.28 | 0.7978 | 0.180 | 5.58 | 30 |
| *AS*-2 | 7.74 | 517 | 1.38 | 0.506 | 1.72 | 0.2466 | 0.316 | 5.50 | 80 |
| *AS*-3 | 11.05 | 362 | 1.38 | 0.330 | 1.29 | 0.0679 | 0.316 | 5.50 | 80 |
| *AS*-4 | 10.21 | 392 | 1.38 | 0.235 | 1.07 | 0.0248 | 0.316 | 5.50 | 80 |
| Brass | | | | | | | | | |
| *BR*-1 | 10.55 | 379 | 1.31 | 0.193 | 1.04 | 0.0199 | 0.250 | 5.25 | 20 |
| *BR*-4 | 10.61 | 377 | 1.28 | 0.156 | 1.09 | 0.0208 | 0.300 | 5.10 | 16 |

[a] All dimensions given in inches; for *A* shells: $E = 10 \times 10^6$ psi, $\nu = 0.3$ for *B* shells: $E = 15.3 \times 10^6$ psi, $\nu = 0.3$

was increased and the scanning process repeated until buckling occurred. The total load and the load distribution was read by 24 strain gages on a load cell. The circumferential load distribution was made as uniform as possible by individually adjusting the four loading screws of the testing machine. A typical load distribution was plus or minus ten percent of the mean load.

The lightly ring-stiffened shells and the stringer-stiffened shells all buckled suddenly with a loud snap. The heavily ring-stiffened shells exhibited a more gentle type of buckling. However, even in these cases the maximum load was easily detected. Typical postbuckling patterns are shown in Fig. 3. The experimental buckling loads are summarized in Table 2. The *A* shells are aluminum and the *B* shells are brass. Ring-stiffened shells are designated with an *R* and stringer-stiffened shells with an *S*.

The theoretical buckling loads for the test shells were calculated considering several different effects and using a variety of analytical methods. However, all the analyses employed assumed that the shell was perfect and the main effort was concentrated on best simulating the experimental conditions. The buckling loads as predicted by classical linear analysis are given in Table 2 under the column headed *SS*-3. For the ring-stiffened shells the lowest load corresponded to an axisymmetric mode. The number of axial half-waves was between 18 and 22 for these shells. The effect of axial constraint was determined for asymmetric buckling modes using the boundary conditions *C*-3 ($w = w_{,x} = v = N_x = 0$) and *C*-4 ($w = w_{,x} = v = u = 0$). These results are shown in

**Table 2 Experimental and theoretical buckling loads (lb/in.)[a]**

| | Theory Prebuckling Analysis | | | | | |
|---|---|---|---|---|---|---|
| | | Membrane | | Nonlinear | | |
| Shell | *SS*-3 | *C*-3 | *C*-4 | *C*-4 | Experiment | Ratio $\rho$ |
| *AR*-1 | 143.2 | 145.1 | 145.3 | 143.2 | 117.7 | 0.822 |
| *AR*-2 | 149.7 | 151.5 | 151.6 | 149.4 | 137.5 | 0.921 |
| *AR*-3 | 174.6 | 176.7 | 177.2 | 174.7 | 148.6 | 0.852 |
| *AR*-4 | 187.2 | 189.5 | 190.0 | 187.0 | 160.9 | 0.862 |
| *AR*-5 | 122.1 | 123.7 | 124.0 | 121.9 | 108.4 | 0.890 |
| *AR*-6 | 123.9 | 125.5 | 125.8 | 123.8 | 109.3 | 0.884 |
| *AR*-7 | 115.4 | 116.7 | 116.9 | 116.0 | 85.8 | 0.740 |
| *AR*-9 | 136.0 | 138.1 | 139.6 | 138.0 | 127.1 | 0.923 |
| *AR*-10 | 149.8 | 152.1 | 153.7 | 150.9 | 132.6 | 0.880 |
| *AR*-11 | 133.3 | 135.3 | 137.0 | 136.0 | 151.9 | 1.116 |
| *AR*-12 | 206.7 | 209.7 | 211.2 | 207.8 | 220.7 | 1.064 |
| *AS*-2 | 123.8 | | 183.8 | 185.6 | 129.2 | 0.697 |
| *AS*-3 | 219.8 | | 290.2 | 285.7 | 200.3 | 0.703 |
| *AS*-4 | 173.5 | | 213.9 | 208.1 | 152.0 | 0.731 |
| *BR*-1 | 281.7 | | 284.1 | 281.5 | 228.5 | 0.813 |
| *BR*-4 | 280.3 | | 281.0 | 280.4 | 196.0 | 0.700 |

[a] Buckling loads ($N_x$) lb/in. *SS*-3, $w = v = N_x = M_x = 0$; *C*-3, $w = v = N_x = \partial w/\partial x = 0$; *C*-4, $w = v = u = \partial w/\partial x = 0$.

**Table 3 Discreteness effect for ring-stiffened shells**

| Shell | $q$ | $m$ | $(q+1)/m$ | $N_x$, smeared | $N_x$, discrete | $\Delta N_x$, % | $N_x$, local |
|---|---|---|---|---|---|---|---|
| *AR*-1[a] | 5 | 5 | 1.2 | 143.2 | 141.9 | 0.92 | 151.2 |
| *AR*-5[a] | 5 | 5 | 1.2 | 122.1 | 118.0 | 3.24 | 118.4 |
| *AR*-9[a] | 5 | 5 | 1.2 | 136.0 | 119.8 | 12.0 | 114.6 |
| *AR*-12[a] | 7 | 5 | 1.6 | 206.7 | 206.0 | 0.35 | 331.5 |

[a] Same geometrical properties as in Table 1 except for length of shell.

columns two and three of Table 2. This additional constraint makes very little difference.

The influence of nonlinear prebuckling deformation was studied for asymmetric modes and compared in columns three and four of Table 2. Again this effect is found to make little difference. The loads reported corresponded to modes with many axial half-waves (16 or more) but few circumferential waves.

Since the number of rings in the test specimens is very close to the number of axial half-waves in the predicted axisymmetric buckle pattern, a recheck on the discreteness effect was made with the theory of Ref. 22. In order to facilitate computations and permit higher order terms to be included, the calculations are carried out for shorter shells (with 5–7 rings instead of 20–30 in the actual test specimens) keeping all other dimensions identical. The results for 4 typical shells are given in Table 3.

These results reconfirm that the discreteness effect is usually small in ring-stiffened shells under axial compression even when the number of ring spacings (number of rings plus one) is very close to the number of axial half-waves in the predicted buckling pattern. The exception occurs when the rings are strong enough to give dominance to local buckling. The discrete theory then yields buckling loads very close to the local buckling loads. When these are considerably lower than the general instability loads an appreciable discreteness effect occurs (*AR*-9, *AR*-5; see footnote to Table 1).

Local buckling between the rings was also reconsidered based on the final measured dimension of the shells. It was found that the shells *AR*-9 and *AR*-10 were prone to local buckling. For the shells *AR*-5, *AR*-6, *AR*-7, and *BR*-4, the local buckling and general instability were close to the same load. However, this type of buckling was not observed on any shell except perhaps *AR*-9. The prebuckling growth, which will be discussed next, showed an axisymmetric pattern on *AR*-9 that might have been caused by buckling between rings.

The analysis of the stringer-stiffened shells using the classical linear theory showed that the lowest buckling load corresponded to a mode with one half axial wave and 9 or 10 circumferential waves. The details of the end ring supports for the shell (Fig. 4) were examined to find the effect of the elastic constraints. It was found that the experimental end conditions were rigid enough to consider the shell fully clamped (*C*-4). Considering this boundary condition, the loads are shown in the third column for the linear prebuckling analysis and column four including the effect of the prebuckling restraint caused by the end rings. As can be seen, the effect of the nonlinear prebuckling deformation is very small. The buckling mode considering this effect was slightly changed from the classical linear theory but always had 10 or more circumferential waves and a few axial half-waves. It was also noted from the analysis that the eigenvalues were fairly close together and care had to be exercised not to miss them in the analysis.

The ratio of experimental load to analysis (using the analysis considering nonlinear prebuckling deformation and *C*-4 boundary conditions) is given in the last column of Table 2. For the ring-stiffened shells this ratio is plotted against the ring area parameter in Figure 5.

The displacement reading for the initial imperfection and the prebuckling growth were recorded on punched cards during the test. Data reduction was done on an IBM 360-75 using the procedure described in detail in Ref. 10. The cards containing the measured deviations from the perfect shell at different load levels were used to prepare three-dimensional plots of the imperfection scans at different load levels by offsetting the origin of the successive circumferential scans

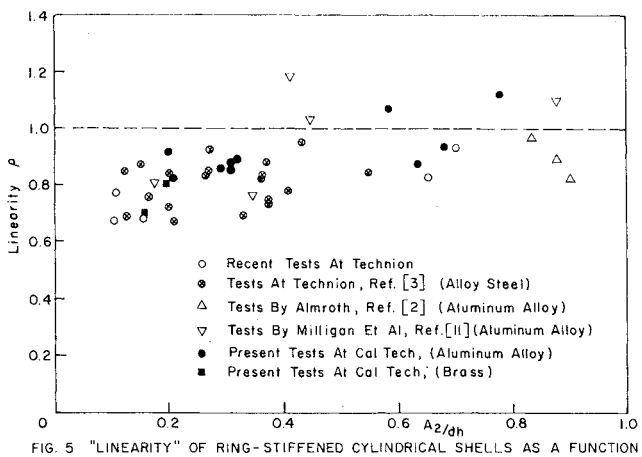


FIG. 5 "LINEARITY" OF RING-STIFFENED CYLINDRICAL SHELLS AS A FUNCTION OF RING AREA

**Fig. 5 Linearity of ring-stiffened cylindrical shells as a function of ring area.**

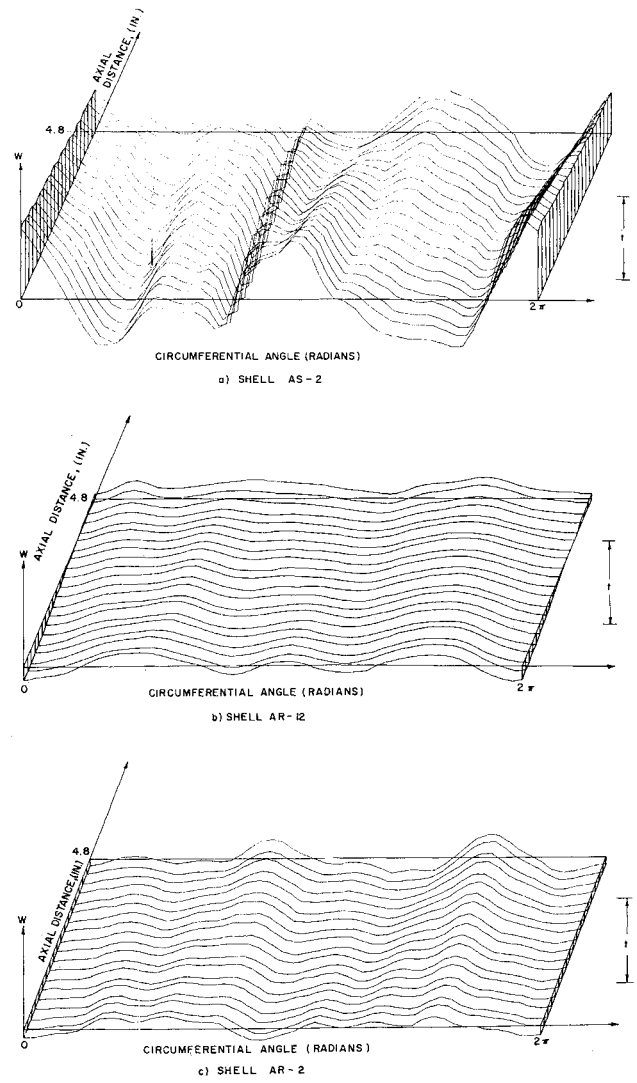


**Fig. 6 Initial imperfection measurements.**

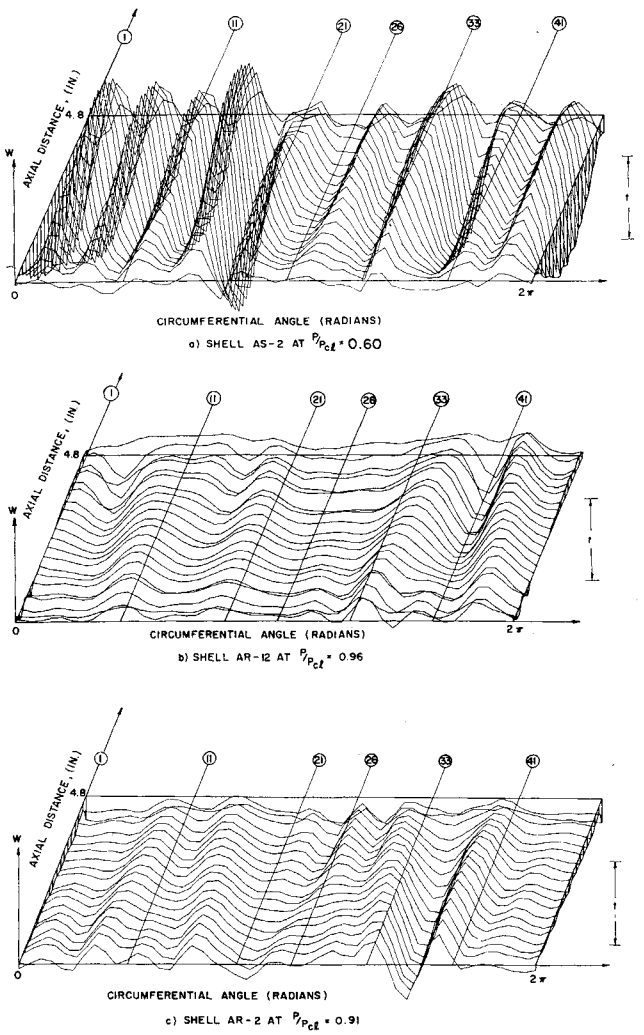


**Fig. 7 Prebuckling deformation growth.**

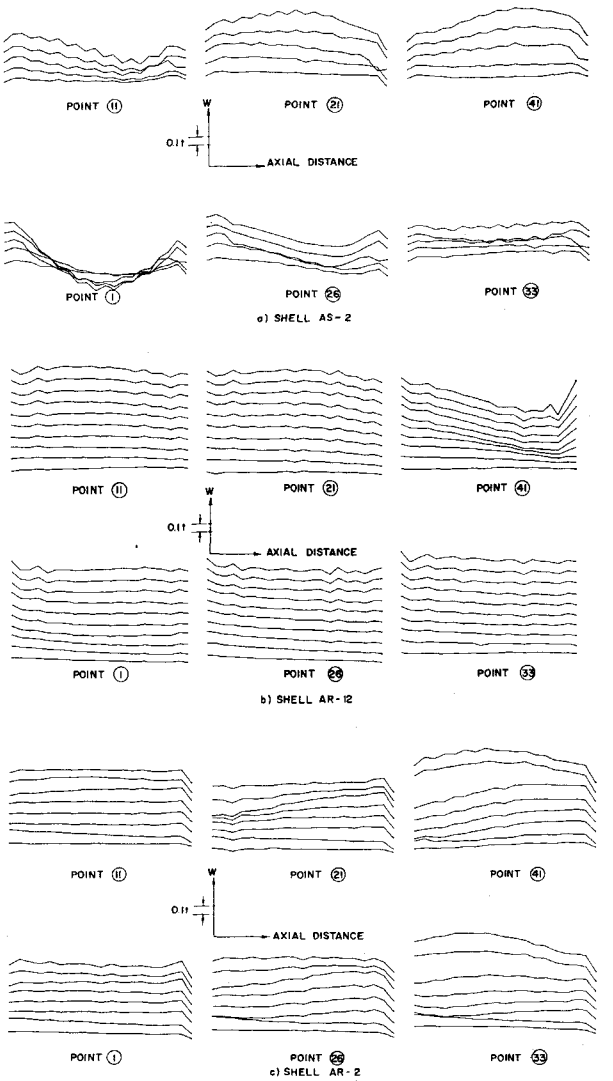


**Fig. 8 Axial cross-plots of the prebuckling deformation growth at increasing load levels.**

by the proper amount along both the $x$ and $y$ axis. The same program was also used to prepare three-dimensional plots of the growth of imperfections at increasing load levels. This was done by subtracting from the measured shell surface at each load level the measured initial imperfections of the shell before calling the plotting subroutine.

The results of the initial imperfection surveys for some typical ring- and stringer-stiffened shells are shown in Fig. 6. As can be seen the ring-stiffened shells $AR$-2 and $AR$-12 have less initial imperfection than the stringer-stiffened shell $AS$-2. Comparing these results with a corresponding plot for the the isotropic shell $A$-12, reproduced here from Ref. 10 as Fig. 7, shows that the stiffened shells are less imperfect.

The three-dimensional plots of the prebuckling deformations show at a glance the general deformation pattern of the shells before buckling. As can be seen from Fig. 8, at the last load level prior to buckling there was a very pronounced growth of an imperfection with one half-wave in the axial direction and several waves in the circumferential direction for both the stringer-stiffened shell $AS$-2 and the lightly ring-stiffened shell $AR$-2. This behavior closely resembles that of isotropic shells as reported in Ref. 10 and repeated here for $A$-12 in Fig. 7. For heavier rings, shell $AR$-12, the prebuckling growth was of an entirely different nature, showing significant axisymmetric contributions. In order to illustrate this axisymmetric contribution more clearly at different circumferential stations, cross plots in the axial directions were drawn. Figure 9 shows clearly that only the heavily ring-stiffened shell $AR$-12 shows definite axisymmetric growth at increasing load levels. However, it is interesting to notice that the prebuckling growth of even the heavily ring-stiffened shell $AR$-12 includes several waves in the circumferential direction.

In an attempt to gain insight into the growth pattern of the prebuckling deformations, harmonic analysis of the measured imperfection surfaces were carried out at each load level. Using a half wave sine axial representation this involved the determination of two sets of harmonic components:

$$\bar{w}(x,y) = \sum_{m=0}^{N}\sum_{n=1}^{N} C_{mn}\cos\frac{my}{R}\sin\frac{n\pi x}{L} + \sum_{m=1}^{N}\sum_{n=1}^{N} D_{mn}\sin\frac{my}{R}\sin\frac{n\pi x}{L} \quad (2)$$

An auxiliary program then computed the growth of each of the coefficients with increasing loading. Figure 10 shows the rate of growth of some of these coefficients.

It is interesting to note that the asymmetric prebuckling growth shown for $AR$-2 and $AS$-2 is about five times the growth found for the isotropic shell.[10] However, the character of the curves is very similar. The axisymmetric component shown for $AR$-12 is much smaller but shows a definite asymptotic type growth near the experimental buckling load. This is the first time that this type of growth was detected for an axisymmetric component.

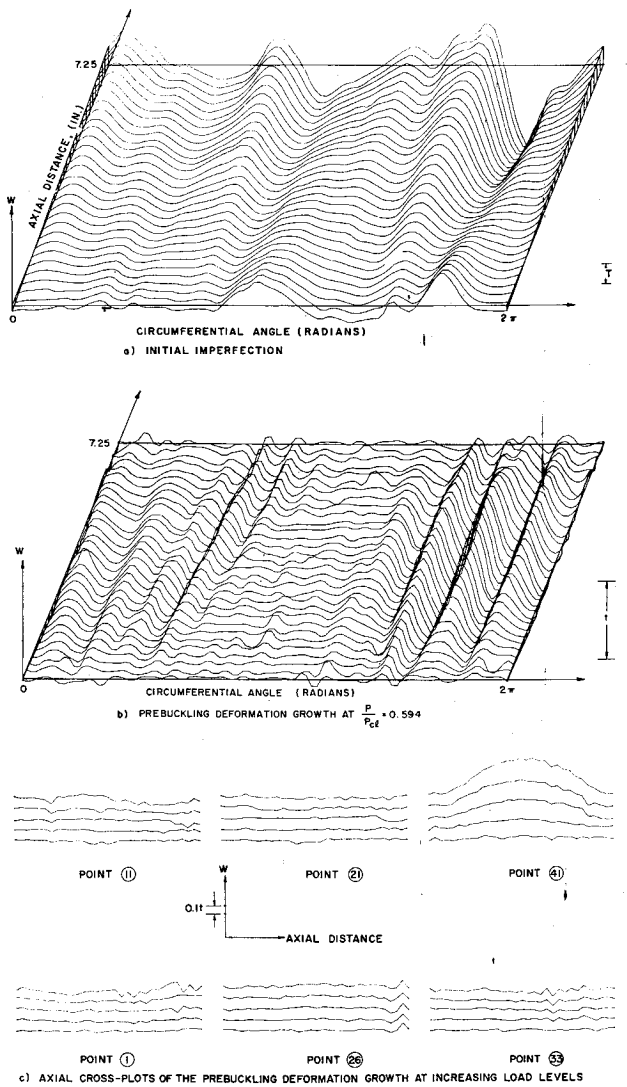


**Fig. 9 Results for the isotropic shell *A*-12.**

## Conclusions

The following conclusions can be drawn from the results obtained so far. Because of the small number of shells these conclusions are preliminary and should be verified by additional tests.

### Ring-Stiffened Shell

1) The initial imperfections of the shells surveyed are of lower order modes (one half-wave in the axial direction and three to five waves in the circumferential direction) and of very small amplitude (only about $\frac{2}{10}$ of the wall thickness). These mode shapes are similar to the earlier results obtained for isotropic shells,[10] which however were of considerably larger amplitudes (about three times the wall thickness). Note that though ring-stiffened shells have an entirely axisymmetric geometry and hence one would expect mostly axisymmetric imperfections, the observed imperfection pattern is predominantly asymmetric!

2) For lightly ring-stiffened shells the prebuckling growth is similar to that of isotropic shells (one half-wave in the axial direction and seven to eight waves in the circumferential direction). This is due to the fact that for lightly ring-stiffened shells asymmetric buckling modes yield only slightly higher buckling loads than the lowest one corresponding to the axisymmetric mode. Thus, the predominantly asymmetric initial imperfections are very strongly amplified.

3) For heavily ring-stiffened shells, the prebuckling growth contains a short wave length axisymmetric component in addition to the usual asymmetric component of one half-wave in the axial direction and about six to seven waves in the circumferential direction. Now for heavily ring-stiffened shells the lowest asymmetric buckling load with one half axial wave is considerably higher than the lowest one corresponding to the axisymmetric mode. Thus, both asymmetric and axisymmetric initial imperfections are amplified.

4) Whereas prebuckling growth extended practically over the entire shell, the postbuckling deformations of the diamond type are usually restricted to part of the shell. The number of circumferential waves in the postbuckling pattern exceeds slightly that of the dominant prebuckling growth.

5) Linearity (correlation with predictions of classical linear theory) is above 80% for most of the shells tested. Linearity is noticeably higher for heavier rings.

6) When local buckling predominates in a closely ring stiffened cylindrical shell, the pattern is axisymmetric and exhibits stable initial postbuckling behavior.

### Stringer-Stiffened Shells

1) Once again the initial imperfections are of lower order modes (one half-wave in the axial direction and about three to four waves in the circumferential direction) but they are of considerably larger amplitude than for the ring stiffened shells (about one wall thickness).

2) There is a very strong prebuckling growth of one half-wave in the axial direction and nine circumferential waves. The dominant prebuckling growth is in a mode that corresponds to a buckling load which is very close to the lowest one predicted by the linear theory.

3) Postbuckling deformations do not differ much from the dominant prebuckling growth. The number of circumferential waves exceeds by one that of the dominant prebuckling growth and axially the buckles cover just about the whole length of the shell.

4) "Linearity" is lower than for ring stiffened shells when correlated with predictions for fully clamped ends.

From the results obtained so far, it appears that the uniqueness of the linear theory buckling mode for perfect stiffened shells influences the prebuckling behavior of imperfect stiffened shells only for relatively heavy stiffening. Thus, an analysis based on the nonlinear interaction of harmonic components, similar to the one carried out for isotropic shells[10] appears feasible and desirable. Such an analysis might help to explain why some lightly ring-stiffened and stringer-stiffened shells buckled at relatively low values of axial loading.

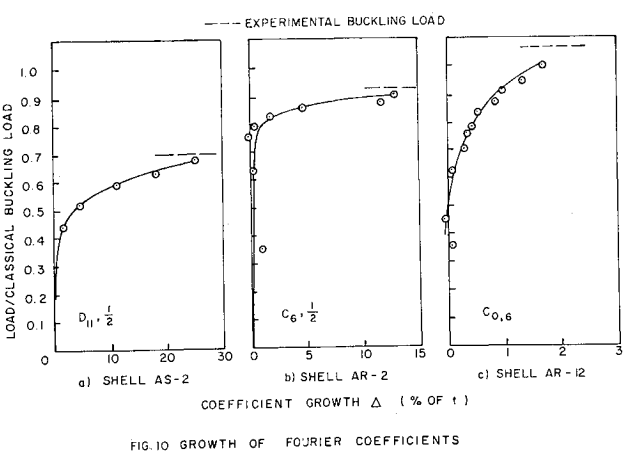


**Fig. 10 Growth of Fourier coefficients.**

## References


[1] Hoff, N. J., "The Perplexing Behavior of Thin Circular Cylindrical Shells in Axial Compression," Second Theodore von Kármán Memorial Lecture, *Proceedings of the 8th Israel Annual Conference on Aviation and Astronautics, Israel Journal of Technology*, Vol. 4, No. 1, Feb. 1966, pp. 1–28.

[2] Almroth, B. O., "Influence of Imperfections and Edge Restraint on the Buckling of Axially Compressed Cylinders," *AIAA/ASME 7th Structures and Materials Conference, AIAA*, New York, 1966; also, CR-432, April 1966, NASA.

[3] Singer, J., "The Influence of Stiffener Geometry and Spacing on the Buckling of Axially Compressed Cylindrical and Conical Shells," *Theory of Thin Shells*, Springer-Verlag, Berlin, 1969, pp. 234–263; also TAE Rept. 68, Oct. 1967, Technion Research and Development Foundation, Haifa, Israel.

[4] Koiter, W. T., "On the Stability of Elastic Equilibrium," Ph.D. thesis (in Dutch), Delft, H. J. Paris, Amsterdam, 1945; also TT F-10, March 1967, NASA, p. 833.

[5] Koiter, W. T., "Elastic Stability of Postbuckling Behavior," *Non-Linear Problems*, edited by R. E. Langer, The University of Wisconsin Press, Madison, Wis., 1963, pp. 257–275.

[6] Koiter, W. T., "The Effect of Axisymmetric Imperfections on the Buckling of Cylindrical Shells under Axial Compression," *Proceedings of the Royal Netherlands Academy of Sciences*, Amsterdam, Ser. B, Vol. 66, No. 5, 1963, pp. 265–279.

[7] Hutchinson, J., "Axial Buckling of Pressurized Imperfect Cylindrical Shells," *AIAA Journal*, Vol. 3, No. 8, Aug. 1965, pp. 1461–1466.

[8] Budiansky, B., "Postbuckling Behavior of Cylinders in Torsion," *Theory of Thin Shells*, Springer-Verlag, Berlin, 1969, pp. 212–233; also Rept. SM-17, Harvard Univ., Cambridge, Mass., Aug. 1967.

[9] Hutchinson, J. W. and Amazigo, J. C., "Imperfection Sensitivity of Eccentrically Stiffened Cylindrical Shells," *AIAA Journal*, Vol. 5, No. 3, March 1967, pp. 392–401.

[10] Arbocz, J. and Babcock, C. D., "The Effect of General Imperfections on the Buckling of Cylindrical Shells," *Journal of Applied Mechanics*, Ser. E, Vol. 36, No. 1, 1969, pp. 28–38.

[11] Milligan, R. et al., "General Instability of Orthotropic Stiffened Cylinders under Axial Compression," *AIAA Journal*, Vol. 4, No. 11, Nov. 1966, pp. 1906–1913.

[12] Card, M. F. and Jones, R. M., "Experimental and Theoretical Results for Buckling of Eccentrically Stiffened Cylinders," TN D-3639, Oct. 1966, NASA.

[13] Katz, L., "Compression Tests on Integrally Stiffened Cylinders," TM X55315, Aug. 1965, NASA.

[14] Len'ko, O. N., "The Stability of Orthotropic Cylindrical Shells," *Raschet Prostranstvennykh Konstruksii*, Issue IV, Moscow, 1958, pp. 499–524, Translation: TT F-9826, July 1963, NASA.

[15] Weller, T., Singer, J., and Nachmani, S., "Recent Experimental Studies on Buckling of Integrally Stiffened Cylindrical Shells under Axial Compression," TAE Rept. 100, Feb. 1970, Technion Research and Development Foundation, Haifa, Israel.

[16] Baruch, M. and Singer, J., "Effect of Eccentricity of Stiffeners on the General Instability of Stiffened Cylindrical Shells under Hydrostatic Pressure," *Journal of Mechanical Engineering Science*, Vol. 5. No. 1, March 1963, pp. 23–27.

[17] Singer, J., Baruch, M., and Harari, O., "On the Stability of Eccentrically Stiffened Cylindrical Shells under Axial Compression," *International Journal of Solids and Structures*, Vol. 3, No. 4, July 1967, pp. 445–470; also TAE Rept. 44, Dec. 1965, Technion Research and Development Foundation, Haifa, Israel.

[18] Seggelke, P. and Geier, B., "Das Beulverhalten versteifter Zylinderschalen Teil 2: Beullasten," *Zeitschrift fur Flugwissenschaft*, Vol. 15, No. 12, 1967, pp. 477–490.

[19] Weller, T. and Baruch, M., "Influence of In-Plane Boundary Conditions on Buckling of Ring Stiffened Cylindrical Shells," TAE Rept. 101, Feb. 1970, Technion Research and Development Foundation, Haifa, Israel.

[20] Bushnell, D., Almroth, B. O., and Sobel, L. H., "Buckling of Shells of Revolution with Various Wall Constructions," Vols. 1–3, CR 1049–1051, 1968, NASA.

[21] Van der Neut, A., "General Instability of Orthogonally Stiffened Cylindrical Shells," *Collected Papers on Instability of Shell Structures—1962*, TN D-1510, Dec. 1962, NASA, pp. 309–319.

[22] Singer, J. and Haftka, R., "Buckling of Discretely Ring Stiffened Cylindrical Shells," *Proceedings of the 10th Israel Annual Conference on Aviation and Astronautics, Israel Journal of Technology*, Vol. 6, Nos. 1–2, Feb. 1968, pp. 125–137; also TAE Rept. 67, Aug. 1967, Technion Research and Development Foundation, Haifa, Israel.

[23] Block, D. L., "Influence of Discrete Ring Stiffeners and Prebuckling Deformations on the Buckling of Eccentrically Stiffened Orthotropic Cylinders," TN D-4283, Jan. 1968, NASA.

[24] Soong, T. C., "Influence of Boundary Constraints on the Buckling of Eccentrically Stiffened Orthotropic Cylinders," Presented at the 7th International Symposium on Space Technology and Science, Tokyo, May 1967.

[25] Almroth, B. O., "Influence of Edge Conditions on the Stability of Axially Compressed Cylindrical Shells," *AIAA Journal*, Vol. 4, No. 1, Jan. 1966, pp. 134–140.

[26] Peterson, J. P., "Buckling of Stiffened Cylinders in Axial Compression and Bending, A Review of Test Data," TN D-5561, Dec. 1969, NASA.

[27] Almroth, B. O. and Bushnell, D., "Computer Analysis of Various Shells of Revolution," *AIAA Journal*, Vol. 6, No. 10, Oct. 1968, pp. 1847–1855.

[28] Kobayashi, S., "The Influence of Prebuckling Deformation on the Buckling Load of Orthotropic Cylindrical Shells under Axial Compression," *Transactions of the Japan Society for Aeronautical and Space Sciences*, Vol. 11, No. 19, 1968, pp. 60–68.

[29] Koiter, W. T., "Buckling and Postbuckling Behavior of a Cylindrical Panel under Axial Compression," Rept. S 476, *Reports and Transactions*, Vol. 20, National Luchtvaartlaboratorium, Amsterdam, The Netherlands 1956.

[30] Brush, D. O., "Imperfection Sensitivity of Stringer Stiffened Cylinders, *AIAA Journal*, Vol. 6, No. 12, Dec. 1968, pp. 2445–2447.

[31] Hutchinson, J. W. and Frauenthal, J. C., "Elastic Postbuckling Behavior of Stiffened and Barreled Cylindrical Shells," *Journal of Applied Mechanics*, Ser. E, Vol. 36, No. 4, Dec. 1969, pp. 784–790.

[32] Tennyson, R. C. and Muggeridge, D. B., "Buckling of Axisymmetric Imperfect Circular Cylindrical Shells under Axial Compression," *AIAA Journal*, Vol. 7, No. 11, Nov. 1969, pp. 2127–2131.